



Published in final edited form as:

Nat Cell Biol. 2013 October ; 15(10): 1153–1163. doi:10.1038/ncb2827.

MicroRNA-205 Controls Neonatal Expansion of Skin Stem Cells by Modulating the PI3K Pathway

Dongmei Wang¹, Zhaojie Zhang^{1,3}, Evan O'Loughlin^{1,3,4}, Li Wang¹, Xiying Fan¹, Eric C. Lai², and Rui Yi^{1,5}

¹Department of Molecular, Cellular, and Developmental Biology, University of Colorado, Boulder, Colorado 80309 USA

²Sloan-Kettering Institute, 1017 Rockefeller Research Labs, 1275 York Avenue Box 252, New York, New York 10065 USA

Abstract

Skin stem cells (SCs) are specified and rapidly expanded to fuel body growth during early development. However, molecular mechanisms that govern the amplification of skin SCs remain unclear. Here we report an essential role for miR-205, one of the most highly expressed miRNAs in skin SCs, in promoting neonatal expansion of these cells. Unlike most mammalian miRNAs, genetic deletion of *miR-205* causes neonatal lethality with severely compromised epidermal and hair follicle growth. In the *miR-205* KO skin SCs, phospho-Akt is significantly downregulated, and the SCs prematurely exit the cell cycle. In the hair follicle, this accelerates the transition of the neonatal SCs towards quiescence. We identify multiple miR-205 targeted negative regulators of PI3K signaling that mediate the repression of phospho-Akt and restrict the proliferation of SCs. Our findings reveal an essential role for miR-205 in maintaining the expansion of skin SCs by antagonizing negative regulators of PI3K signaling.

Tissue stem cells (SCs) are specified during early development. In mouse skin, hair follicle stem cells (HFSCs) emerge between embryonic day 14 (E14) and postnatal day 0.5 (P0.5) at the initiation of hair follicle (HF) morphogenesis¹. These newly specified SCs must undergo proliferative expansion to accommodate body growth and enlargement of individual tissues. In adults, however, HFSCs form a quiescent cell population that infrequently cycle and maintain the SC pool throughout life^{2, 3}. Therefore, there is a transition leading proliferative SCs to exit the cell cycle and become quiescent. During this transition, gene regulatory

Users may view, print, copy, download and text and data- mine the content in such documents, for the purposes of academic research, subject always to the full Conditions of use: http://www.nature.com/authors/editorial_policies/license.html#terms

⁵Correspondence should be addressed to: R.Y. (yir@colorado.edu).

³These authors contributed equally to this work.

⁴Current address: Program in Biological and Biomedical Sciences, Harvard Medical School, Boston, MA 02115 USA

Note: Supplementary Information is available on the Nature Cell Biology Website

Author Contributions

R.Y. conceived the study. D.W. carried out most experiments and analyzed the data with assistance from Z.Z. (bioinformatic analysis), E.O. (*in situ* hybridization), L.W. (ChIP-Seq and RNA-Seq) and X.F. (target validation). E.C.L. provided critical resources. R.Y. and D.W. wrote the manuscript with the input from all authors.

Competing Financial Interests

The authors declare no competing financial interests.

networks balancing output from multiple pathways regulating proliferation, quiescence, survival and cell death must be precisely coordinated^{4, 5}. In skin, the molecular mechanisms governing the transition of SCs from the expansion phase to quiescence remain poorly understood.

MicroRNAs (miRNAs), a class of tiny regulatory RNAs, have been proposed to play important roles in diverse biological processes⁶. However, few studies have specifically addressed the role played by individual miRNAs in the expansion and maintenance of tissue SCs during mammalian development *in vivo*⁷. Although global ablation of the miRNA pathway through genetic deletion of either *Dicer* or *Dgcr8* has provided insights into the requirement of miRNAs in embryonic SCs and tissue development^{8–13}, the pleiotropic defects caused by the loss of hundreds of miRNAs make it impossible to elucidate the underlying mechanisms. Surprisingly, it has not yet been reported that the loss of a single miRNA leads to severe defects either in animal development or in tissue SCs, in contrast to lethal phenotypes often observed in *Dicer* or *Dgcr8* conditional knockout (cKO) animals^{7, 14, 15}. Thus, it remains a major challenge to characterize the functional significance of individual miRNAs in tissue SCs and elucidate their molecular mechanisms.

Here we report that miR-205 is one of the most highly expressed miRNAs in skin SCs. We demonstrate by genetic deletion of *miR-205* that miR-205 is not only essential for mouse development but also specifically required for the expansion of the progenitor and SC populations in both epidermis and HF¹s during neonatal skin development. Furthermore, we provide mechanistic insights into miR-205 function by demonstrating potent regulation of the PI3K pathway. Together, this study establishes a paradigm for the role of individual miRNAs in balancing the proliferation and quiescence of tissue SCs during early development.

Results

miR-205 is highly enriched in skin progenitors and stem cells

We have previously shown that both *Dicer* and *Dgcr8* skin cKO animals exhibit much smaller body size and shortened HF¹s (Supplementary Fig. S1a)^{10, 13}. When we monitored the dynamics of the HFSCs, we observed that HFSC specification was intact in the absence of *Dicer* in the newborn skin, as determined by immunofluorescence (IF) staining of *Nfatc1*^{1, 16} (Supplementary Fig. S1b). However, in P4.5 *Dicer* cKO skin, the *Nfatc1*⁺ HFSC population was absent (Supplementary Fig. S1c) and the *Sox9*⁺ HFSCs and progenitor cells^{1, 17} were also significantly reduced in the bulge (Supplementary Fig. S1d). These observations indicate that global miRNA expression is required for the expansion and self-renewal of HFSCs during neonatal development.

We then performed *in situ* hybridization to determine the expression patterns for 10 most highly expressed miRNAs in neonatal skin¹³. We found that miR-205 is highly enriched in skin progenitors and SCs during skin development (Fig. 1a–e). At E10, when the skin still comprises a single layer of multipotent embryonic skin progenitors, miR-205 was already detectable in the cytoplasm of these *p63*⁺ progenitors¹⁸ (Fig. 1a). At E14, when the basal cells begin to stratify, miR-205 was restricted to the basal progenitors, and was absent from

the differentiating suprabasal cells (Fig. 1b). When the HF lineage begins to emerge from the basal layer, miR-205 was further upregulated in the HF placode (Fig. 1c). When visualized in both neonatal and adult skin, miR-205 was expressed in interfollicular progenitor cells but most highly enriched in the bulge, where HFSCs reside (Fig. 1d,e and Supplementary Fig. S2a).

To quantify the differential expression of miR-205 in the epidermal and HF lineages, we isolated interfollicular progenitors, HFSCs, outer root sheath (ORS) progenitors and transient amplifying Matrix (Mx) cells with a K14-RFP/Sox9-GFP mouse model¹⁹ in P4 skin (Supplementary Fig. S2c). We validated each population by qRT-PCR for well-established marker genes (Fig. 1f). We then determined that miR-205 was expressed at the highest level in the HFSCs, followed by the interfollicular progenitors and the ORS, when compared to the Mx cells (Fig. 1g). When we quantified miR-205 in telogen (P19) and anagen (P28) bulge as $\alpha 6^{\text{hi}}\text{CD}34^{\text{hi}}$ populations²⁰, we observed higher expression in the telogen HFSCs (Supplementary Fig. S2b). Together, our *in situ* and qRT-PCR analyses identify miR-205 as one of the most highly expressed miRNAs in skin progenitors and SCs.

We next determined miR-205's expression among different murine tissues. In a comprehensive survey of miRNA expression patterns in mouse and human, miR-205 was only detected in epithelial tissues that include skin, prostate, and mammary gland²¹. Similarly, when we quantified miR-205 expression in 12 murine tissues obtained from P7.5 animals with qRT-PCR, we found that miR-205 was strongly enriched in stratified epithelial tissues including skin, tongue, bladder and stomach and largely absent from other tissues (Fig. 1h). Furthermore, *in situ* hybridization for miR-205 together with a well-established basal epithelial cell marker, Krt5 (K5) revealed that miR-205 was expressed only in K5+ cells in all tissues examined (Supplementary Fig. S3a–b). Although it remains a possibility that miR-205 may be expressed in rare cell populations in non-epithelial tissues, these data suggest that miR-205 is highly specific for K5+ basal cells within stratified epithelial tissues.

Generation of *miR-205* knockout mouse

The *miR-205* gene is located in an intergenic region on mouse chromosome 1. The primary transcript of *miR-205* has been previously detected in mouse neonatal skin cDNA as a non-coding RNA (AK014513, UCSC genome browser) (Fig. 2a and Supplementary Fig. S4a). By using ChIP-Seq for H3K4me3 and H3K36me3 marks that define actively transcribed genomic regions by RNA polymerase II²², we determined that the primary transcript of *miR-205* was transcribed in E14 basal cells (Fig. 2a). With an RNA-Seq specifically for the polyA tail²³, we determined that the primary transcript was polyadenylated using a canonical signal (AUUAAA) (Fig. 2a). Although mature miR-205 sequences are highly conserved in vertebrates, the primary transcript shows poor conservation outside of the *miR-205* hairpin (Supplementary Fig. S4). We then generated a *miR-205* KO mouse model (Fig. 2b–d) and validated the complete ablation of miR-205 by qRT-PCR and *in situ* (Fig. 2e).

miR-205 knockout mouse is neonatal lethal

miR-205 KO animals were born with the expected Mendelian ratio [WT:het:KO=137(22%):328(53%):156(25%)]. Whereas the KO animals were indistinguishable in appearance from their WT or heterozygous littermates at birth, by P5 they became weaker and had less well-developed hair coats (Fig. 3a). miR-205 KO animals usually died ~10 days after birth, whereas the heterozygous animals showed no sign of any defects and were indistinguishable from their WT littermates. Therefore, the loss of miR-205 has dire consequences leading to neonatal lethality, unlike many individual miRNA KOs that are apparently normal and lack obvious developmental defects¹⁴. We investigated miR-205 in the skin because of the clear similarities in the miR-205 KO and the Dicer skin cKO animals, and because of the high miR-205 levels in skin. At P4.5, the miR-205 KO skin developed thinner epidermis (Fig. 3b). The HFs were short and also mis-angled, similar to the HFs that grow downward in the Dicer cKO (Fig. 3c). The terminal differentiation of both epidermal and HF lineages in the miR-205 KO was not dramatically altered, as judged by IF staining of skin lineage markers (Supplementary Fig. S5). Furthermore, these animals did not exhibit any discernible barrier defects (Fig. 3d). We did not observe any evaginating HFs and apoptotic cells, hallmarks of the Dicer cKO skin^{9, 10}, suggesting that the absence of other miRNAs may be responsible for these defects.

Ablation of miR-205 impairs the proliferation of interfollicular progenitors

To examine the interfollicular progenitors²⁴, we bred *miR-205*^{+/-} to *K14-RFP* mice so that we could identify the progenitors by $\alpha 6^{\text{hi}}$ /RFP^{hi} expression in the epidermal fraction after separating the epidermis from HFs (Supplementary Fig. S2c). The miR-205 KO progenitors exhibited significantly reduced proliferation compared to their WT counterparts using BrdU cell cycle analysis. Whereas an average of 35.7% of the progenitors were BrdU⁺ in the WT, only 12.6% were BrdU⁺ in the miR-205 KO (Fig. 4a). Therefore, the compromised proliferation likely contributes to the thinner epidermis, as well as the smaller skin surface of miR-205 KO animals (Fig. 4b). To further document the proliferation defects *in vivo*, we used Ki67 staining to distinguish cells that were in active cell cycle from those that exited the cell cycle. At P4.5, 88.9% of interfollicular progenitors were positive for Ki67 in the WT skin. In contrast, only 52.3% of progenitors were positive for Ki67 in the miR-205 KO skin. By P7.5, 55.1% of interfollicular progenitors were positive for Ki67 in the WT, whereas the Ki67 positive population dropped to 24.9% in the miR-205 KO skin (Fig. 4c). To distinguish whether these defects were intrinsic to the loss of miR-205 in the skin or due to systemic effects, we grafted WT and KO skin onto nude mice (Supplementary Fig. S6). In agreement with the cell-autonomous role of miR-205, the transplanted KO skin showed much less Ki67⁺ cells than the WT skin (Fig. 4d,e).

We next isolated the interfollicular progenitors from both WT and KO skin and compared their colony formation capacity *in vitro*. We observed a strong reduction in the formation of large, holoclonal colonies by miR-205 KO progenitors even though the total number of colonies was similar (Fig. 4f). Collectively, these data suggest that the loss of miR-205 directly compromises the proliferation and leads to premature cell cycle exit in the interfollicular progenitors.

Ablation of miR-205 compromises the proliferation of progenitors and stem cells in hair follicles

In the HF lineage, BrdU analysis revealed that the HFSCs and ORS progenitor cells were also less proliferative in the KO skin (Fig. 5a,b). In contrast, the transient amplifying Mx cells were equally proliferative between the WT and KO samples (Fig. 5c). Because miR-205 is highly enriched in the HFSCs and ORS but not in the Mx cells, these data indicate that the loss of miR-205 specifically compromises the proliferation of the progenitors and HFSCs. Consistent with the impaired cell cycle progression, when we quantified the HFSC population by IF staining for Nfatc1 or Sox9, miR-205 KO showed a mild but statistically significant reduction in the number of HFSCs (Fig. 5d,e). This indicates that the compromised proliferation leads to a smaller HFSC population in the absence of miR-205. The diminished SC and ORS progenitor population likely reduced the supply for transient amplifying Mx cells, leading to smaller hair bulbs, even though all Mx cells were still actively cycling in the KO (Fig. 5f).

Unlike interfollicular progenitors, HFSCs in adult skin are quiescent and only become activated to fuel hair cycle periodically or in response to epidermal wound repair^{3, 24, 25}. However, HFSCs are specified during hair morphogenesis¹ and they must undergo neonatal expansion before entering quiescence. Because the deletion of miR-205 causes impaired HFSC proliferation, we asked whether miR-205 plays a key role in the transition from proliferation to quiescence. We first monitored the dynamics of newly specified HFSCs as marked by Nfatc1 during embryonic skin development^{1, 16, 17}. At E17.5, all of these nascent HFSCs were actively cycling as indicated by strong Ki67 signals in the newly formed hair germ (Supplementary Fig. S7a). At P0.5, all of these HFSCs were still Ki67+, reflecting a continuous expansion of the HFSC population to fuel HF growth (Supplementary Fig. S7b). By P1.5, however, a few Nfatc1+ HFSCs especially those in mature HFs began to lose Ki67 signals, marking the onset of the transition towards quiescence (Supplementary Fig. S7c). By P4.5, 47.5% of the WT HFSCs lost Ki67 signal and transitioned towards quiescence. In contrast, 68.4% of the miR-205 KO HFSCs lost Ki67 signal and became quiescent (Fig. 5g). Furthermore, reduced HFSC proliferation led to the accumulation of label-retaining cells in the KO bulge in a BrdU pulse/chase experiment (Fig. 5h). Together, these analyses suggest the possibility that miR-205 KO HFSCs prematurely exit the cell cycle and transition towards quiescence.

While miR-205 is most highly expressed in HFSCs, it is also expressed in the ORS. As expected, we observed a dramatic decrease in Ki67+ cells in the miR-205 KO ORS (Fig. 5i). The ORS cells constitute the major portion of the HF in length, such that their reduced proliferation likely contributed to the shortened HFs as seen in the KO skin. Taken together, these *in vivo* results provide insights for the requirement for miR-205 to maintain cell proliferation in neonatal HFSCs and progenitors.

We next isolated HFSCs from WT and miR-205 KO skin and compared their colony formation capacity *in vitro*. We first confirmed that both WT and KO cells had similar plating efficiency (Fig. 5j). Importantly, miR-205 KO HFSCs showed significantly compromised colony formation capacity such that the number of large holoclones was

dramatically reduced (Fig. 5k). Altogether, these findings demonstrate that miR-205 is intrinsically required for the proliferation of HFSCs both *in vivo* and *in vitro*.

Ablation of miR-205 impairs the proliferation of basal cells in stratified epithelium

Because miR-205 was detected in K5+ basal cells in other stratified epithelium located in oesophagus and tongue (Supplementary Fig. S3a), we examined the cell proliferation in these tissues. As expected, the proliferation of K5+ basal cells in oesophagus and tongues was also compromised, as judged by both Ki67 and BrdU labeling (Fig. 6). These results indicate a general requirement for miR-205 in K5+ basal cells of the stratified epithelium. Furthermore, compromised proliferation in multiple stratified epithelial tissues could contribute to the lethality of miR-205 KO animals.

miR-205 directly targets multiple negative regulators of the PI3K pathway

To identify direct targets of miR-205, we isolated the HFSCs from WT and miR-205 KO skin at P4 and compared mRNA expression by microarray analysis. We identified 201 genes that were consistently upregulated more than 20% in miR-205 KO samples in two sets of biological duplicates. We performed a motif search for all possible 7mers that are represented in the miR-205 sequences in the 5' UTR, coding region and 3'UTR of these genes. We found that only the 1-7, 2-8 and 3-9 seed motifs, which are located at the 5' end of miR-205, were significantly enriched only in the 3'UTRs of the upregulated genes (Fig. 7a and Supplementary Fig. S8a-c). As a control, we did not observe any enrichment for any 7mer motif represented by miR-1 (Supplementary Fig. S8d). These results indicate, as expected, that miR-205 selectively represses the expression of genes that bear its seed sequences in their 3'UTR. Out of 201 upregulated genes, 96 genes (47.8%) contain at least one miR-205 seed match in their 3'UTR (Supplementary Table 1). Collectively, these results support the cell-autonomous role of miR-205 in modulating gene expression in the HFSCs.

We performed a pathway analysis for these 96 genes²⁶ and identified *tumor suppressor* as the most significantly enriched SwissProt/PIR keyword. Derepression of tumor suppressor genes (TSGs) is known to inhibit self-renewal and reduce stem cell populations²⁷⁻²⁹. In our list, APC, Frk, Inpp4b and Phlda3 are known TSGs³⁰⁻³². We also identified Inpp1, a known negative regulator in the PI3K pathway³³, which is a previously identified miR-205 target in human keratinocytes^{34, 35}. To validate these targets, we first determined the 3' UTR for each gene using our RNA-Seq database generated from the HFSCs and then tested their responsiveness to miR-205 by insertion 3' to a luciferase indicator gene, with both WT and mutated miR-205 seed sequences (Supplementary Fig. S8e). Four of five genes were robustly regulated by miR-205 as demonstrated by derepressed luciferase activity when the miR-205 target site(s) was mutated (Fig. 7b). Among these targets, Phlda3 and Inpp1 were abundantly expressed and we further validated their upregulation at the protein level by Western blotting with FACS purified interfollicular progenitors and HFSCs (Fig. 7c). When we used the purified Mx cells as a control, we did not detect Phlda3 in either WT or KO cells and we did not observe upregulation of Inpp1 in the KO Mx cells. These data confirm the specific regulation of these targets by miR-205 in interfollicular progenitors and HFSCs.

To provide more insights into the expression pattern of miR-205 and its target mRNAs, we isolated HFSCs and measured their expression level by qRT-PCR during embryonic/neonatal development. Interestingly, the expression of both miR-205 and these targets gradually increased from E17.5 to P3.5 and P10.5 (Fig. 7d). This result suggests that miR-205 is upregulated to balance the enhanced expression of these TSGs.

miR-205 is required for the maintenance of pAkt levels

We noted that Frk, Inpp4b, Inpp11 and Phlda3 all negatively regulate the PI3K/Akt pathway^{30–33}. This prompted us to examine pAkt levels in the skin. Strikingly, the pAkt levels were significantly downregulated in interfollicular progenitors (90%), HFSCs (86%) and ORS (38%) but only slightly in the Mx cells (18%) in miR-205 KO skin (Fig. 8a). To ensure that the downregulation of pAkt was specific to these skin lineages and not due to systemic defects in the miR-205 KO animals, we measured pAkt levels in other vital organs including brain, brown fat, heart and lung, and observed normal pAkt levels (Supplementary Fig. S8f). Intriguingly, pAkt was also significantly downregulated in the Dicer cKO epidermis (95%) (Fig. 8b). These results suggest that miR-205 is specifically required to maintain pAkt levels in the progenitors and SCs in skin.

The level of pAkt has been directly linked to the proliferation and self-renewal of skin SCs^{36–38}. When we blocked pAkt using a small molecule inhibitor of PI3K in cultured keratinocytes, the growth of primary keratinocytes was abolished (Supplementary Fig. S8g). To test whether the derepression of miR-205 targets, including Inpp4b, Frk, Phlda3 and Inpp11, dampens the PI3K/Akt pathway, we infected primary keratinocytes with MSCV vectors expressing each of these genes. Upon enhanced expression of these targets, pAkt levels were downregulated (Fig. 8c) and cell proliferation was compromised (Fig. 8d). Interestingly, the ability to inhibit growth by these regulators correlated with their ability to reduce pAkt levels. This suggests that high pAkt levels are closely associated with proliferative capacity. Finally, to test whether the downregulation of pAkt contributes primarily to the growth defects caused by the loss of miR-205, we infected the miR-205 KO HFSCs with a constitutively active Akt mutant (myr-Akt) and evaluated the colony formation capacity. As expected, myr-Akt largely rescued the growth defects of freshly isolated miR-205 KO HFSCs (Fig. 8e). Taken together, these results argue that miR-205 co-represses multiple negative regulators of the PI3K/Akt pathway and, by doing so, miR-205 maintains a high pAkt level that promotes the proliferation and expansion of progenitors and SCs in developing skin (Fig. 8f).

Discussion

miRNAs have been implicated important roles in gene regulation in mammalian SCs^{7, 39–41}. However, genetic KO models in either *C. elegans* or mouse have implicated very few individual miRNAs as indispensable for animal development^{14, 15, 42}. Here we report that miR-205 plays an essential role in promoting their expansion during early development. This provides one of the first examples in which genetic deletion of a single miRNA causes severe developmental defects and compromises the function of tissue SCs.

Our study also provides additional insights into the transition of neonatal HFSCs from the active cycling state to quiescence. We identify a network of negative regulators of the PI3K pathway that are directly targeted by miR-205. During skin development, the expression of these negative regulators and miR-205 increases concurrently. Upon the loss of miR-205, negative regulators of the PI3K pathway become prematurely elevated and reduce pAkt levels. Reduced pAkt levels then compromises the proliferation of the progenitor and SC populations in the skin. However, the proliferation defect alone does not likely cause the lethality. We note that miR-205 has been implicated important roles in the regulation of cell adhesion and migration^{43, 44}. Positive regulators of cell migration e.g. Arhgap5 and Cxcl12 are also identified as targets of miR-205 (Supplementary Table S1). It is an intriguing possibility that potential defects in cell migration could contribute to the severe developmental defects.

Methods

Methods and any associated references are available in the online version of the paper.

Supplementary Material

Refer to Web version on PubMed Central for supplementary material.

Acknowledgments

We are grateful to E. Fuchs for *K14-RFP* mice. We thank T. Blumenthal, T. Cech, B. Cullen, M. Han, M. Winey and X-J. Wang for comments on the manuscript. We thank C. Yang, J. Gao, D. Feng for the generation of *miR-205* knockout; S. Ha and L. Greiner for assistance in the animal facility; Y. Han for FACS; and G. Voeltz for confocal microscopy. We also thank members of the Yi lab for their critical discussions. This publication was made possible by a start-up fund provided by the University of Colorado and Grant Number R00AR054704 and R01AR059697 (R.Y.) and R01GM083300 (E.C.L.).

References

1. Nowak JA, Polak L, Pasolli HA, Fuchs E. Hair follicle stem cells are specified and function in early skin morphogenesis. *Cell Stem Cell*. 2008; 3:33–43. [PubMed: 18593557]
2. Cotsarelis G, Sun TT, Lavker RM. Label-retaining cells reside in the bulge area of pilosebaceous unit: implications for follicular stem cells, hair cycle, and skin carcinogenesis. *Cell*. 1990; 61:1329–1337. [PubMed: 2364430]
3. Tumber T, et al. Defining the epithelial stem cell niche in skin. *Science*. 2004; 303:359–363. [PubMed: 14671312]
4. He S, Nakada D, Morrison SJ. Mechanisms of stem cell self-renewal. *Annu Rev Cell Dev Biol*. 2009; 25:377–406. [PubMed: 19575646]
5. Hsu YC, Fuchs E. A family business: stem cell progeny join the niche to regulate homeostasis. *Nat Rev Mol Cell Biol*. 2012; 13:103–114. [PubMed: 22266760]
6. Bartel DP. MicroRNAs: target recognition and regulatory functions. *Cell*. 2009; 136:215–233. [PubMed: 19167326]
7. Yi R, Fuchs E. MicroRNAs and their roles in mammalian stem cells. *J Cell Sci*. 2011; 124:1775–1783. [PubMed: 21576351]
8. Murchison EP, Partridge JF, Tam OH, Cheloufi S, Hannon GJ. Characterization of Dicer-deficient murine embryonic stem cells. *Proc Natl Acad Sci U S A*. 2005; 102:12135–12140. [PubMed: 16099834]
9. Andl T, et al. The miRNA-processing enzyme dicer is essential for the morphogenesis and maintenance of hair follicles. *Curr Biol*. 2006; 16:1041–1049. [PubMed: 16682203]

10. Yi R, et al. Morphogenesis in skin is governed by discrete sets of differentially expressed microRNAs. *Nat Genet.* 2006; 38:356–362. [PubMed: 16462742]
11. Wang Y, Medvid R, Melton C, Jaenisch R, Blleloch R. DGCR8 is essential for microRNA biogenesis and silencing of embryonic stem cell self-renewal. *Nat Genet.* 2007; 39:380–385. [PubMed: 17259983]
12. Melton C, Judson RL, Blleloch R. Opposing microRNA families regulate self-renewal in mouse embryonic stem cells. *Nature.* 2010; 463:621–626. [PubMed: 20054295]
13. Yi R, et al. DGCR8-dependent microRNA biogenesis is essential for skin development. *Proc Natl Acad Sci U S A.* 2009; 106:498–502. [PubMed: 19114655]
14. Liu N, Olson EN. MicroRNA regulatory networks in cardiovascular development. *Dev Cell.* 2010; 18:510–525. [PubMed: 20412767]
15. Small EM, Olson EN. Pervasive roles of microRNAs in cardiovascular biology. *Nature.* 2011; 469:336–342. [PubMed: 21248840]
16. Horsley V, Aliprantis AO, Polak L, Glimcher LH, Fuchs E. NFATc1 balances quiescence and proliferation of skin stem cells. *Cell.* 2008; 132:299–310. [PubMed: 18243104]
17. Hsu YC, Pasolli HA, Fuchs E. Dynamics between stem cells, niche, and progeny in the hair follicle. *Cell.* 2011; 144:92–105. [PubMed: 21215372]
18. Senoo M, Pinto F, Crum CP, McKeon F. p63 Is essential for the proliferative potential of stem cells in stratified epithelia. *Cell.* 2007; 129:523–536. [PubMed: 17482546]
19. Zhang L, Stokes N, Polak L, Fuchs E. Specific MicroRNAs Are Preferentially Expressed by Skin Stem Cells To Balance Self-Renewal and Early Lineage Commitment. *Cell Stem Cell.* 2011; 8:294–308. [PubMed: 21362569]
20. Blanpain C, Lowry WE, Geoghegan A, Polak L, Fuchs E. Self-renewal, multipotency, and the existence of two cell populations within an epithelial stem cell niche. *Cell.* 2004; 118:635–648. [PubMed: 15339667]
21. Landgraf P, et al. A mammalian microRNA expression atlas based on small RNA library sequencing. *Cell.* 2007; 129:1401–1414. [PubMed: 17604727]
22. Guttman M, et al. Chromatin signature reveals over a thousand highly conserved large non-coding RNAs in mammals. *Nature.* 2009; 458:223–227. [PubMed: 19182780]
23. Wang L, Dowell RD, Yi R. Genome-wide maps of polyadenylation reveal dynamic mRNA 3'-end formation in mammalian cell lineages. *RNA.* 2013; 19:413–425. [PubMed: 23325109]
24. Blanpain C, Fuchs E. Epidermal stem cells of the skin. *Annu Rev Cell Dev Biol.* 2006; 22:339–373. [PubMed: 16824012]
25. Ito M, et al. Stem cells in the hair follicle bulge contribute to wound repair but not to homeostasis of the epidermis. *Nat Med.* 2005; 11:1351–1354. [PubMed: 16288281]
26. Huang da W, Sherman BT, Lempicki RA. Bioinformatics enrichment tools: paths toward the comprehensive functional analysis of large gene lists. *Nucleic Acids Res.* 2009; 37:1–13. [PubMed: 19033363]
27. Park IK, et al. Bmi-1 is required for maintenance of adult self-renewing haematopoietic stem cells. *Nature.* 2003; 423:302–305. [PubMed: 12714971]
28. Ezhkova E, et al. EZH1 and EZH2 cogovern histone H3K27 trimethylation and are essential for hair follicle homeostasis and wound repair. *Genes Dev.* 2011; 25:485–498. [PubMed: 21317239]
29. Cheng T, et al. Hematopoietic stem cell quiescence maintained by p21cip1/waf1. *Science.* 2000; 287:1804–1808. [PubMed: 10710306]
30. Gewinner C, et al. Evidence that inositol polyphosphate 4-phosphatase type II is a tumor suppressor that inhibits PI3K signaling. *Cancer Cell.* 2009; 16:115–125. [PubMed: 19647222]
31. Yim EK, et al. Rak functions as a tumor suppressor by regulating PTEN protein stability and function. *Cancer Cell.* 2009; 15:304–314. [PubMed: 19345329]
32. Kawase T, et al. PH domain-only protein PHLDA3 is a p53-regulated repressor of Akt. *Cell.* 2009; 136:535–550. [PubMed: 19203586]
33. Dyson JM, et al. The SH2 domain containing inositol polyphosphate 5-phosphatase-2: SHIP2. *Int J Biochem Cell Biol.* 2005; 37:2260–2265. [PubMed: 15964236]

34. Yu J, et al. MicroRNA-184 antagonizes microRNA-205 to maintain SHIP2 levels in epithelia. *Proc Natl Acad Sci U S A*. 2008; 105:19300–19305. [PubMed: 19033458]
35. Yu J, et al. MicroRNA-205 promotes keratinocyte migration via the lipid phosphatase SHIP2. *FASEB J*. 2010; 24:3950–3959. [PubMed: 20530248]
36. Alonso L, et al. Sgk3 links growth factor signaling to maintenance of progenitor cells in the hair follicle. *J Cell Biol*. 2005; 170:559–570. [PubMed: 16103225]
37. Murayama K, et al. Akt activation induces epidermal hyperplasia and proliferation of epidermal progenitors. *Oncogene*. 2007; 26:4882–4888. [PubMed: 17297448]
38. Kobiela K, Stokes N, de la Cruz J, Polak L, Fuchs E. Loss of a quiescent niche but not follicle stem cells in the absence of bone morphogenetic protein signaling. *Proc Natl Acad Sci U S A*. 2007; 104:10063–10068. [PubMed: 17553962]
39. Gangaraju VK, Lin H. MicroRNAs: key regulators of stem cells. *Nat Rev Mol Cell Biol*. 2009; 10:116–125. [PubMed: 19165214]
40. Ivey KN, Srivastava D. MicroRNAs as regulators of differentiation and cell fate decisions. *Cell Stem Cell*. 2010; 7:36–41. [PubMed: 20621048]
41. Martinez NJ, Gregory RI. MicroRNA gene regulatory pathways in the establishment and maintenance of ESC identity. *Cell Stem Cell*. 2010; 7:31–35. [PubMed: 20621047]
42. Miska EA, et al. Most *Caenorhabditis elegans* microRNAs are individually not essential for development or viability. *PLoS Genet*. 2007; 3:e215. [PubMed: 18085825]
43. Gregory PA, et al. The miR-200 family and miR-205 regulate epithelial to mesenchymal transition by targeting ZEB1 and SIP1. *Nat Cell Biol*. 2008; 10:593–601. [PubMed: 18376396]
44. Li C, Finkelstein D, Sherr CJ. Arf tumor suppressor and miR-205 regulate cell adhesion and formation of extraembryonic endoderm from pluripotent stem cells. *Proc Natl Acad Sci U S A*. 2013; 110:E1112–1121. [PubMed: 23487795]

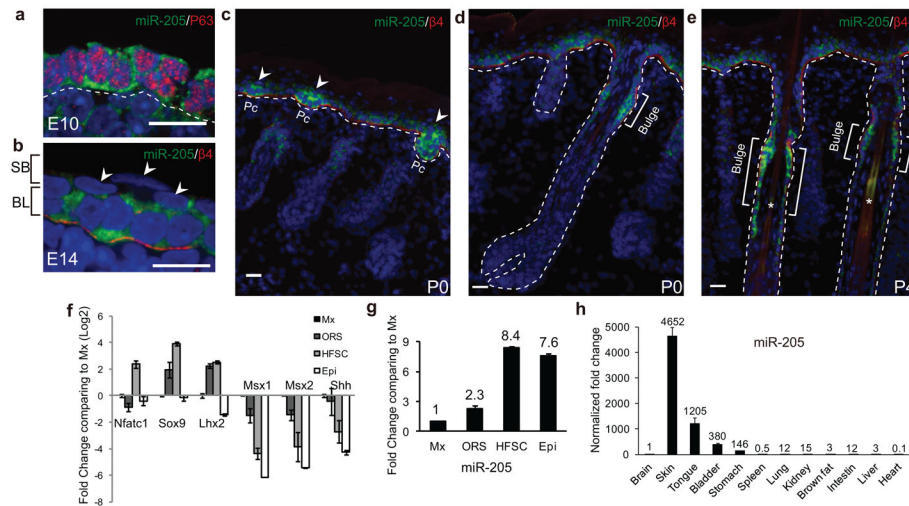


Figure 1. miR-205 is highly expressed in skin progenitors and SCs. **(a)** At E10, miR-205 is expressed in embryonic skin SCs that also express high levels of p63. Note the cytoplasmic localization of miR-205 signals. **(b)** At E14, miR-205 is restricted in the basal SCs. Arrowheads point to the differentiated, suprabasal cells that are negative for miR-205. The basement membrane is marked by $\beta 4$ integrin. SB, suprabasal layer; BL, basal layer. **(c)** miR-205 is upregulated in the HF placode (Pc, arrowheads) but also expressed in interfollicular progenitors in the newborn skin (P0). Note more intense signal of miR-205 in the HF placode than in the interfollicular epidermis. **(d and e)** miR-205 is most highly expressed in the HFSCs located in the bulge of mature HFs. Brackets denote the bulge region. **(f)** FACS-purified populations are validated by qRT-PCR. Data shown are mean \pm s.d. collected from 3 independent experiments. **(g)** Comparing to Matrix (Mx), miR-205 is highly enriched in HFSCs, followed by interfollicular progenitors (Epi) and ORS, as determined by qRT-PCR. Data shown are mean \pm s.d. collected from 3 independent experiments. **(h)** miR-205 is highly enriched in organs containing stratified epithelial tissue, in contrast to a very low or non-detectable level in most of other vital organs. Data shown are mean \pm s.d. collected from 3 independent experiments. All of the data are normalized to Sno25. Numbers indicate normalized fold change. Statistics source data for Fig. 1f–h can be found in Table S2. White dotted lines mark the epidermal/dermal boundary. **a, b**, confocal images; **c, d, e**, epifluorescence images. Scale bars, 20 μ m.

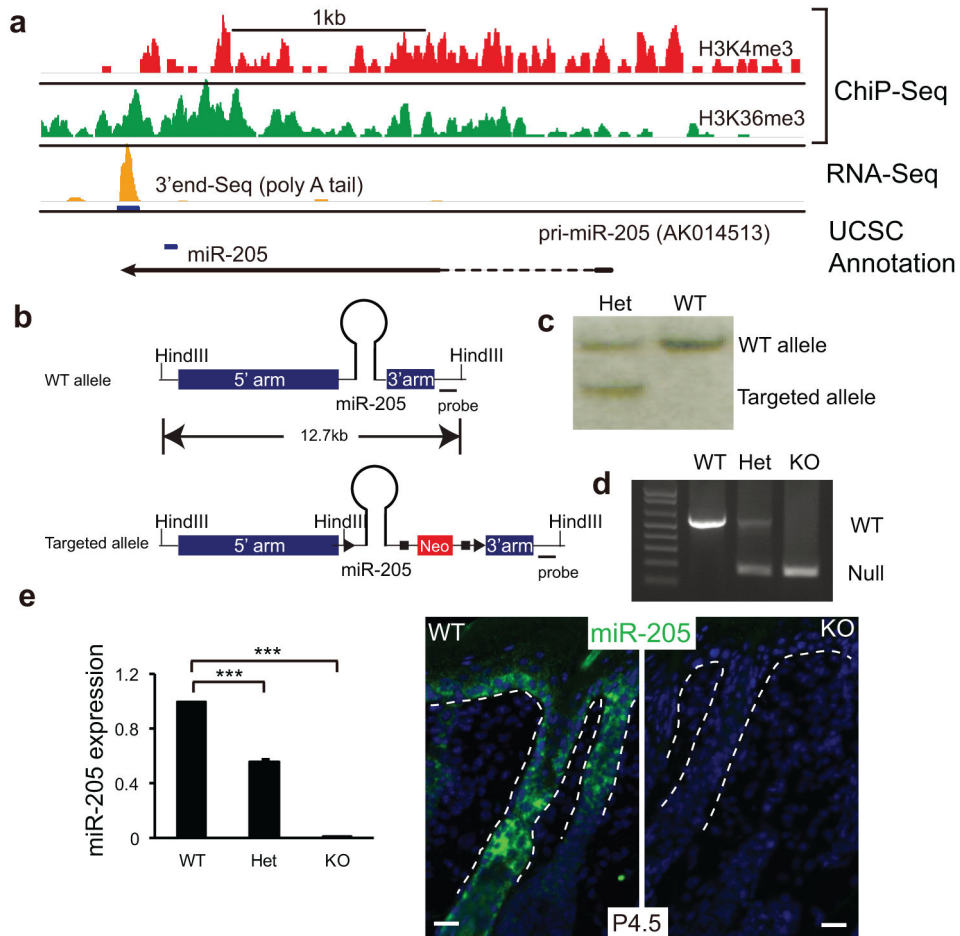


Figure 2. Generation of miR-205 knockout mice. **(a)** Genomic analysis of the *miR-205* locus in embryonic skin progenitor cells: H3K4me3 and H3K36me3 ChIP-Seq data define the actively transcribed region. 3'end sequencing of polyA RNAs detects the polyadenylation site of the primary transcript of *miR-205*. The blue bar denotes the position of the *pre-miR-205* hairpin in the *pri-miR-205* transcript. **(b)** Structure of the WT and targeted *miR-205* locus. **(c)** Southern blot analysis confirms the generation of the targeted allele. **(d)** PCR analysis confirms genotypes. **(e)** Depletion of miR-205 is determined by qRT-PCR and *in situ* hybridization. Data shown are mean \pm s.d. collected from five independent experiments. ***, $P < 0.001$ by Student's *t*-test. White dotted lines mark the epidermal/dermal boundary.

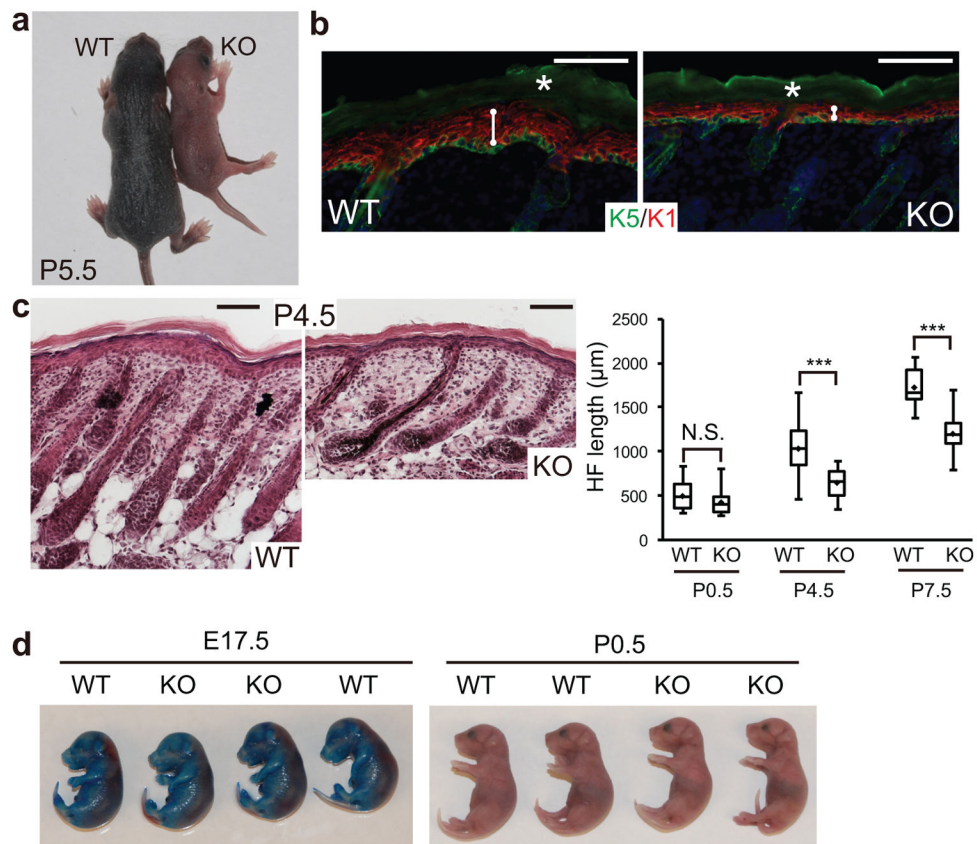
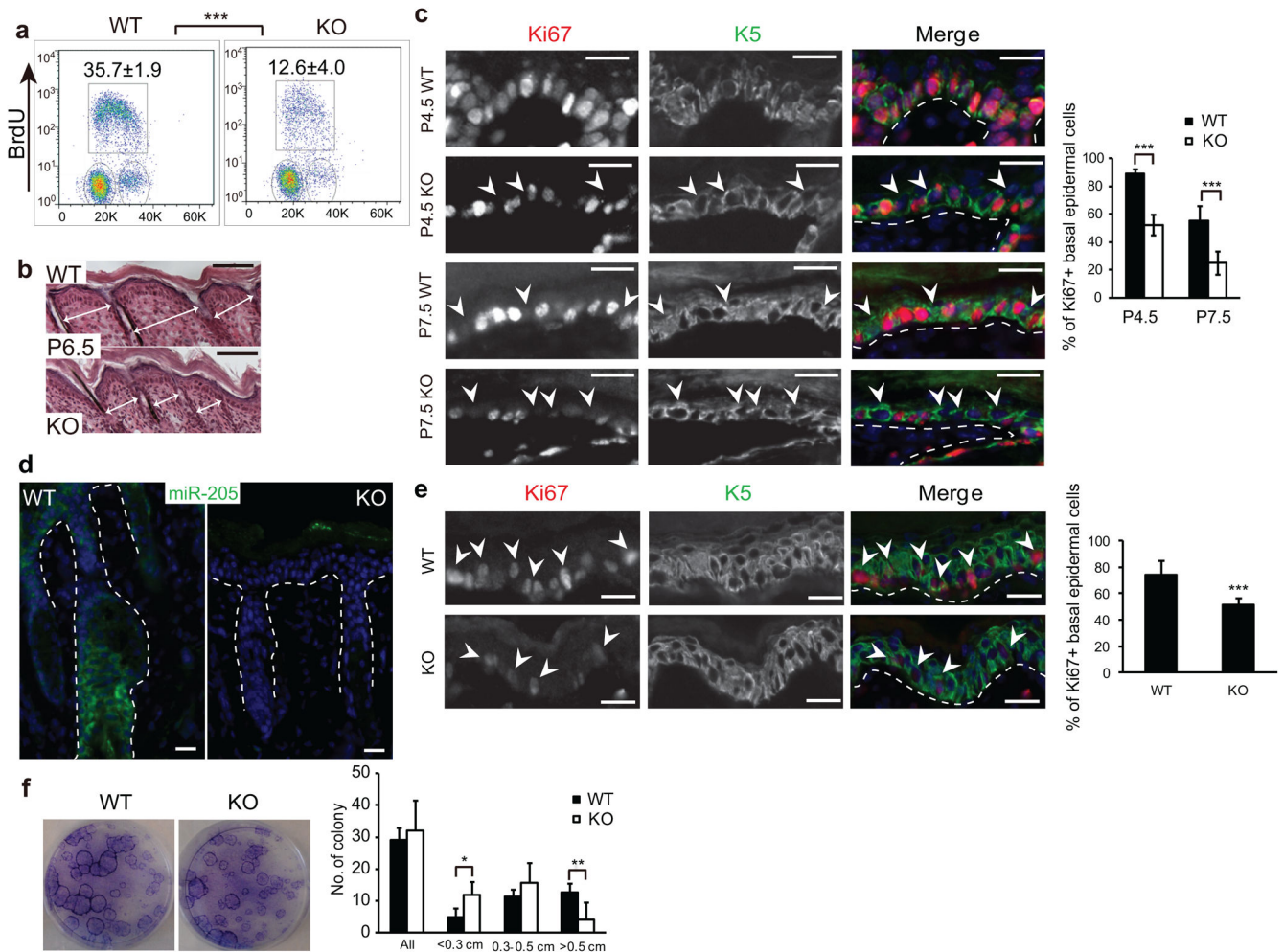


Figure 3. Genetic deletion of miR-205 causes neonatal lethality with severe skin defects. **(a)** At P5.5, the miR-205 KO pup is smaller and shows less developed hair coat, indicated by less pigmentation, compared with the WT littermate. **(b)** miR-205 KO skin shows thinner epidermis. K5 labels the basal layer and K1 labels the spinous layer. White lines measure the thickness of the epidermis; white asterisks denote autofluorescence. **(c)** Shorter HFs are developed in the KO skin. Box and whisker plots quantify the HF length: minimum and maximum lengths are marked by the whiskers; upper and lower boundaries indicate 25 and 75 quartile divisions; central lines indicate median; diamonds indicate average. Data shown are mean \pm s.d., $n = 20$ HFs from 5 pairs of WT and KO littermates. ***, $P < 0.001$ by Student's *t*-test. **(d)** miR-205 deletion does not cause barrier defects as indicated by the toluidine blue dye penetration assay. Scale bars in **b** and **c**, 100 μ m.

**Figure 4.**

Ablation of miR-205 compromises the proliferation of interfollicular progenitors. **(a)** Ablation of miR-205 results in a marked decline in S-phase cells that incorporate BrdU in the basal epidermis. Values are mean \pm s.d. from five independent experiments; ^{***}, $P < 0.001$ by Student's t -test. **(b)** The KO skin shows shortened distance between HFs, an indication of less proliferative epidermis. White arrows measure the distance between adjacent HFs. **(c)** miR-205 KO interfollicular progenitors prematurely exit the cell cycle, as indicated by significantly decreased Ki67+ cells in the basal epidermis. White dotted lines mark the epidermal/dermal boundary; arrowheads indicate K5+/Ki67- interfollicular progenitors. Data shown are mean \pm s.d. from five independent experiments; ^{***}, $P < 0.001$ by Student's t -test. **(d)** *In situ* hybridization confirms the complete loss of miR-205 in the grafted KO skin. **(e)** Fifteen days after grafting onto nude mice, the miR-205 KO epidermis is much less proliferative as indicated by less Ki67+ interfollicular progenitors and thinner epidermis. Data shown are mean \pm s.d. from five independent experiments; ^{***}, $P < 0.001$ by Student's t -test. **(f)** miR-205 KO primary epidermal keratinocytes show a significant reduction in the formation of large holoclones *in vitro*. Data shown are mean \pm s.d. from five

independent experiments. *, $P < 0.05$; **, $P < 0.01$ by Student's t -test. Scale bar is 100 μm in **b** and 20 μm in **c**, **d** and **e**.

Author Manuscript

Author Manuscript

Author Manuscript

Author Manuscript

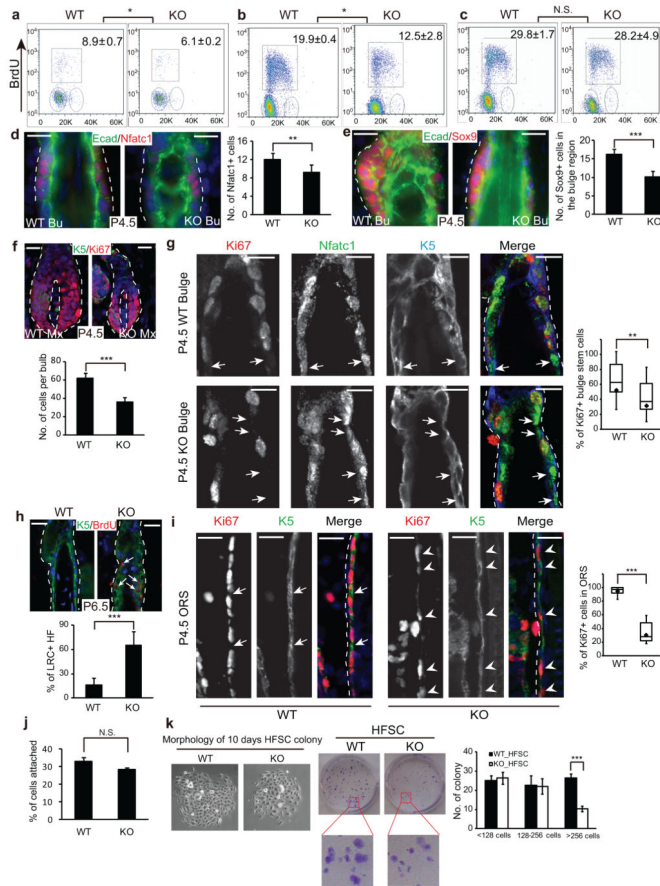


Figure 5. miR-205 is required for the expansion of HFSCs during neonatal development. (a–c) Ablation of miR-205 results in a marked decline in S-phase cells that incorporate BrdU in the HFSCs (a) and ORS progenitors (b), but does not affect the matrix cells (c). Values are mean \pm s.d. from 5 independent experiments. *, $P < 0.05$. N.S., not significant. (d and e) Reduced HFSC population in the miR-205 KO bulge is shown by Nfatc1 and Sox9 staining. Bu, bulge. Data shown are mean \pm s.d., $n = 10$ HF from 5 pairs of WT/KO littermates. **, $P < 0.01$; ***, $P < 0.001$. (f) Matrix cells are equally proliferative in the KO and WT, despite the overall reduction of the matrix size. Data shown are mean \pm s.d., $n = 10$ HF from 5 pairs of WT/KO littermates. ***, $P < 0.001$. (g) Nfatc1+ HFSCs prematurely exit the cell cycle and become quiescent upon miR-205 deletion, determined by Ki67 staining. Arrows indicate Nfatc1+/Ki67– quiescent HFSCs. $n = 10$ HF from 5 pairs of WT/KO littermates. **, $P < 0.01$. (h) BrdU pulse/chase experiments show increased label-retaining cells (LRC) in the miR-205 KO bulge. Data shown are mean \pm s.d., $n = 30$ HF from 3 pairs of WT/KO littermates. ***, $P < 0.001$. (i) Many ORS progenitors in the miR-205 KO exit the cell cycle prematurely. Arrows indicate K5+/Ki67– ORS cells in WT; arrowheads indicate K5+/Ki67+ ORS cells that are actively cycling in KO. $n = 10$ HF from 5 pairs of WT/KO littermates. ***, $P < 0.001$. (j) Similar plating efficiency between WT and miR-205 KO HFSCs. (k) miR-205 KO HFSCs show a significant reduction in the formation of large holoclones *in vitro*. Data shown are mean \pm s.d. from 5 independent experiments. ***, $P <$

0.001. For **g** and **i**, box and whisker plots: minimum and maximum are marked by the whiskers; upper and lower boundaries indicate 25 and 75 quartile divisions; central lines indicate median; diamonds indicate average. Statistics for all assays is calculated by Student's *t*-test. Scale bars, 20 μm .

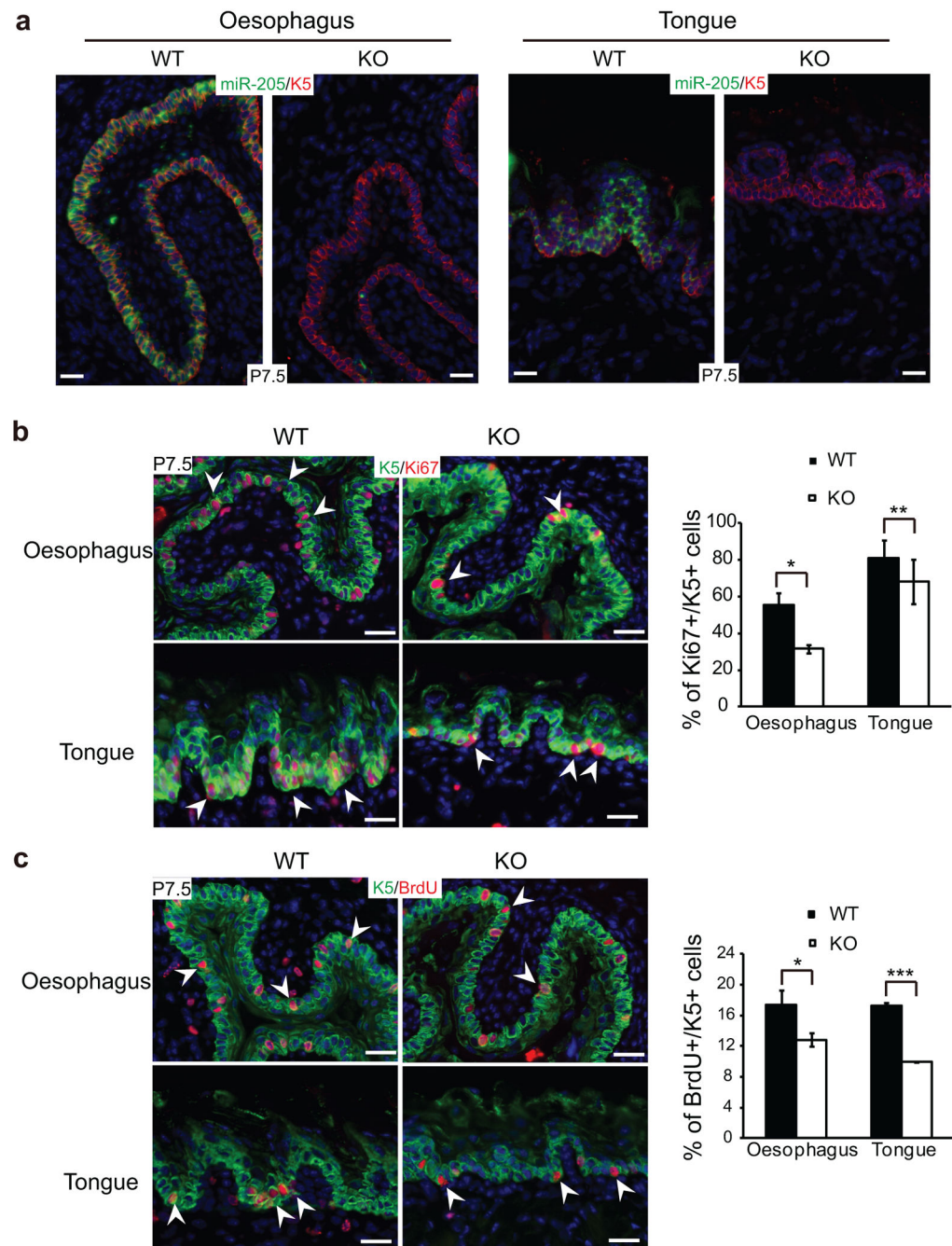
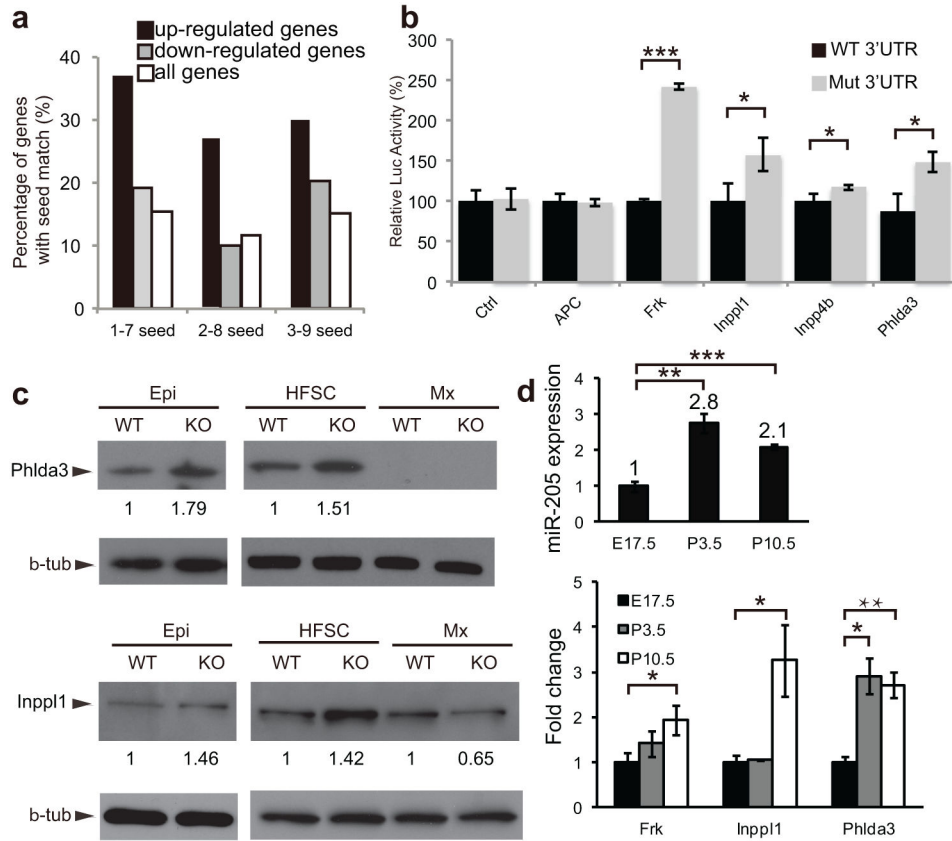
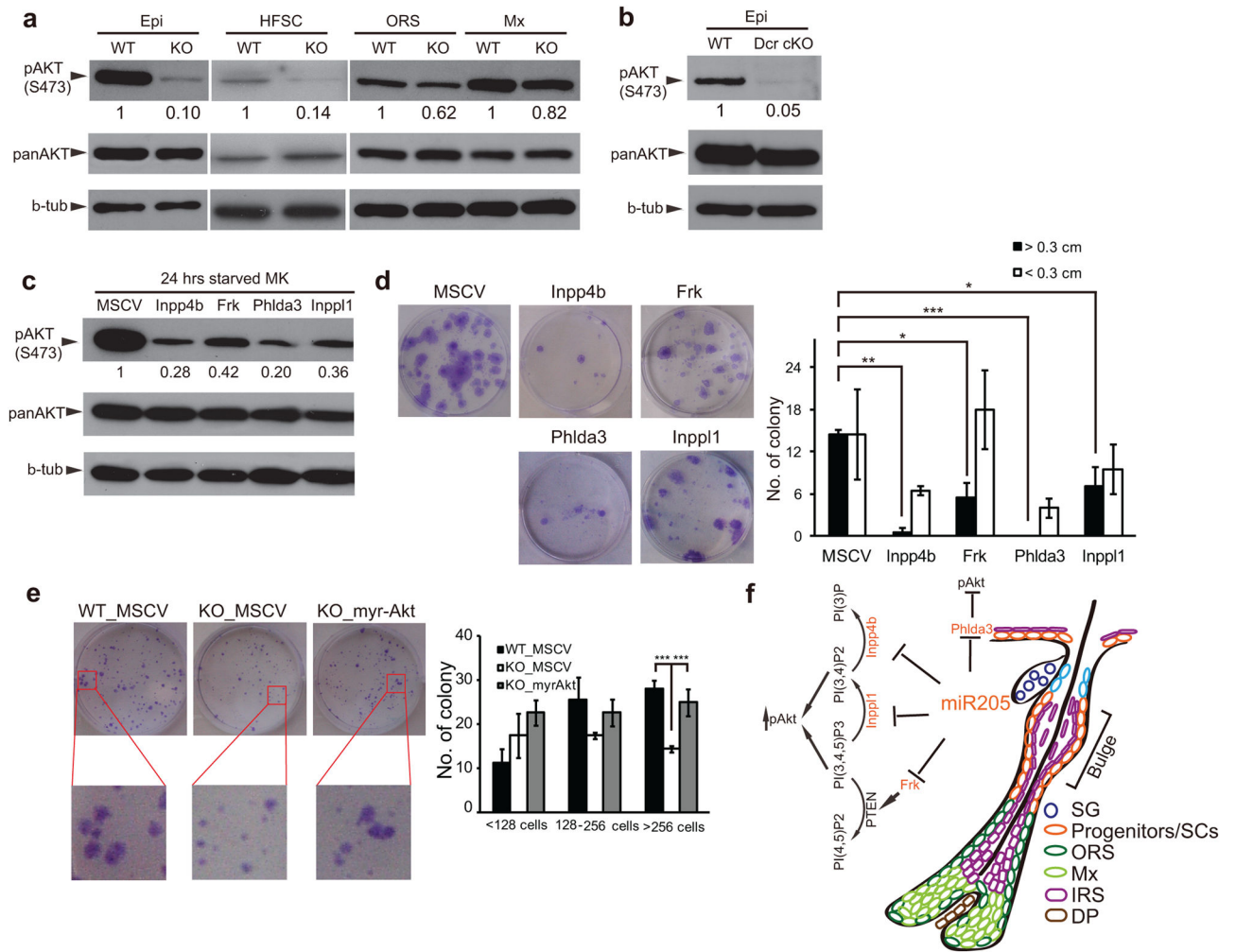


Figure 6.

Ablation of miR-205 impairs the proliferation of K5+ basal cells in stratified epithelium. **(a)** Confirmation of the complete loss of miR-205 in the KO oesophagus and tongue by *in situ* hybridization. **(b and c)** K5+ basal cells are less proliferative as indicated by Ki67 and BrdU staining in the KO oesophagus and tongue. Data shown are mean \pm s.d. from five independent experiments. *, $P < 0.05$; **, $P < 0.01$; ***, $P < 0.001$ by Student's *t*-test.

**Figure 7.**

miR-205 directly targets multiple negative regulators of the PI3K/Akt pathway. **(a)** The enrichment of miR-205 seed matches in the 3'UTR of the upregulated genes in the miR-205 KO HFSCs is shown by a higher percentage of genes containing the seed matches over that of the downregulated or all genes. **(b)** Target validation is shown by the 3'UTR luciferase assay. For control (Ctrl), black and grey bars represent the luciferase activity of pGL3-Ctrl with and without miR-205 transfection, respectively. For the target genes, black bars represent the normalized luciferase activity (set at 100%) of the pGL3-Luc reporter fused with the 3'UTR from each candidate; grey bars represent the derepressed luciferase activity of the pGL3-Luc reporter with mutated miR-205 seed matches in the 3'UTR. Data shown are mean \pm s.d. from six independent experiments. *, $P < 0.05$; ***, $P < 0.001$ by Student's t -test. **(c)** Derepression of miR-205 targets Phlda3 and Inpp1 in miR-205 KO interfollicular progenitors (Epi) and HFSCs. Phlda3 is not detected in either WT or KO matrix (Mx), whereas Inpp1 is not derepressed in miR-205 KO matrix. Numbers between panels represent the densitometry values of target protein normalized to β -tubulin. **(d)** Gradually increased expression of miR-205 and its targets from embryonic stage to postnatal stages is quantified by qRT-PCR. Data shown are mean \pm s.d. from 5 independent experiments. *, $P < 0.05$; **, $P < 0.01$; ***, $P < 0.001$ by Student's t -test. Uncropped images of blots are shown in Supplementary Fig. S9.

**Figure 8.**

miR-205 is required to maintain pAkt levels by targeting multiple negative regulators in skin progenitors and SCs. **(a)** pAkt levels are significantly decreased in miR-205 KO epidermis (Epi), HFSCs and ORS, but only slightly decreased in matrix (Mx). **(b)** pAkt is significantly downregulated in Dicer cKO (Dcr cKO) epidermis (Epi). **(c)** Keratinocytes infected with miR-205 targets (Inpp4b, Frk, Phlda3 and Inpp1) show lower pAkt levels compared to control (MSCV) infected cells. **(d)** Forced expression of individual miR-205 targets compromises the capacity of primary keratinocytes to form productive colonies. Data shown are mean \pm s.d. from five independent experiments. *, $P < 0.05$; **, $P < 0.01$; ***, $P < 0.001$ by Student's *t*-test. **(e)** Constitutively active Akt (myr-Akt) rescues the growth defects of miR-205 KO HFSCs *in vitro*. Data shown are mean \pm s.d. from five independent experiments. ***, $P < 0.001$ by Student's *t*-test. **(f)** A model illustrates the role of miR-205 in the proliferation and expansion of skin progenitors and SCs by antagonizing multiple negative regulators of the PI3K/Akt pathway. Uncropped images of blots are shown in Supplementary Fig. S9.